Presented at the International Conference on
Hyperfine Interactions Studied in Nuclear
Reactions and Decay, Uppsala, Sweden,
June 10-14, 1974.

LBL-3323
c.2

NEGATIVE MUON SPIN ROTATION AND SOLID STATE STUDIES

T. Yamazaki, K. Nagamine, S. Nagamiya, O. Hashimoto,
K. Sugimoto, K. Nakai and S. Kobayashi

August 1974

Prepared for the U. S. Atomic Energy Commission
under Contract W-7405-ENG-48

TWO-WEEK LOAN COPY

This is a Library Circulating Copy which may be borrowed for two weeks. For a personal retention copy, call Tech. Info. Division, Ext. 5545

LAWRENCE BERKELEY LABORATORY
UNIVERSITY OF CALIFORNIA
BERKELEY

LBL-3323 c.2

DISCLAIMER

This document was prepared as an account of work sponsored by the United States Government. While this document is believed to contain correct information, neither the United States Government nor any agency thereof, nor the Regents of the University of California, nor any of their employees, makes any warranty, express or implied, or assumes any legal responsibility for the accuracy, completeness, or usefulness of any information, apparatus, product, or process disclosed, or represents that its use would not infringe privately owned rights. Reference herein to any specific commercial product, process, or service by its trade name, trademark, manufacturer, or otherwise, does not necessarily constitute or imply its endorsement, recommendation, or favoring by the United States Government or any agency thereof, or the Regents of the University of California. The views and opinions of authors expressed herein do not necessarily state or reflect those of the United States Government or any agency thereof or the Regents of the University of California.

NEGATIVE MUON SPIN ROTATION AND SOLID STATE STUDIES†

T. Yamazaki, K. Nagamine, S. Nagamiya, O. Hashimoto, K. Sugimoto, K. Nakai and S. Kobayashi

Department of Physics, University of Tokyo
Bunkyo-ku, Tokyo, Japan

and

Lawrence Berkeley Laboratory
University of California
Berkeley, California 94720

Abstract

The principle of the muon spin rotation method is described with emphasis on possible applications to solid-state studies. Some experimental results of negative muon spin rotation experiments at Lawrence Berkeley Laboratory are given: g factor measurements in diamagnetic metals and relaxation phenomena in transition metals.

1. Introduction

The muon, which is produced in the decay of the pion, has full polarization in the pion rest frame because of the parity violation:

$$\pi^+ \rightarrow \mu^{+\downarrow} + \nu_\mu^{\uparrow}$$
$$\pi^- \rightarrow \mu^{-\uparrow} + \bar{\nu}_\mu^{\downarrow}$$

where arrow ↑ means helicity + 1. The muon itself decays in the following way:

$$\mu^+ \rightarrow e^+ + \nu_e + \bar{\nu}_\mu$$
$$\mu^- \rightarrow e^- + \bar{\nu}_e + \nu_\mu$$

and again because of the parity violation the decay electron shows asymmetry with respect to the muon spin (and thus to the muon direction):

$$W(\theta) = 1 + A \cos \theta \tag{1}$$

The energy averaged coefficient $\bar{A}$ is $\pm \frac{1}{3} P_\mu$ for $\mu^\pm$, respectively. In the presence of a transverse magnetic field the muon spin precesses and the angular asymmetry is perturbed in such a way that

$$W(\theta,t) = 1 + A \cos (\theta-\omega_L t) \tag{2}$$

where

$$\omega_L = - g_\mu \frac{eH}{2m_\mu c} \quad . \tag{3}$$

Such a time differential experiment yields information on the magnetic field at the muon, and this method can be called μSR (muon spin rotation, relaxation, resonance, etc.) corresponding to NMR or ESR.

The first such experiment was done in 1957 by Garwin et al. [1] to show the parity violation in muon decay, and within a few subsequent years novel techniques of precise determination of ω_L, namely, stroboscopy [2], digitization, and even the magnetic resonance [3] in connection with a longitudinal field, were developed. It is rather surprising that the μSR method and the field of "radiative detection of hyperfine interactions" have undergone quite the independent developments. In spite of obvious applicabilities of μSR to solid-state studies, only a few experiments have been done until recently. For the past few years, however, new activities in the field of μSR, especially μ^+SR, have grown up and already some review articles for both μ^+SR and μ^-SR are available [4,5].

The University of Tokyo group has just started μ^-SR experiments in collaboration with the μ^+SR group at Lawrence Berkeley Laboratory in order to explore possibilities to apply to solid-state studies. In the present talk we will give brief sketches of the problems in the μSR method and some preliminary results mainly in μ^-SR.

2. Principle

Table 1 summarizes characteristic features of both μ^+SR and μ^-SR. The following are short comments on each item.

2.1 Spin

The muon has spin of 1/2, and thus detects only magnetic interactions. This is true not only for μ^+, but also for μ^- bound to a spinless nucleus.

2.2 g Factor and Larmor Frequency

The g factor of the positive muon, which is referred to as g_μ^{free}, is well known [6]. It is

$$g_\mu^{free} = \begin{cases} 2.0022 & \text{in units of the muon magneton} \quad (4a) \\ 17.780 & \text{in units of the nuclear magneton.} \quad (4b) \end{cases}$$

The Larmor frequency is

$$f_\mu^{free} = \frac{\omega_\mu}{2\pi} = 13.554 \text{ kHz/Gauss.} \quad (5)$$

The g factor of the negative muon which is bound to a spinless nucleus (hereafter we consider only I = 0 cases) is reduced due to the relativistic correction, but at most by 3-4 percent even for heavy nuclei. This problem will be described in Section 4. In any case, the muon g factor is about 20 times greater than those of typical nuclear magnetic probes. This simply indicates that T_2 due to any field broadening becomes shorter by a factor of 20 and that T_1 due to time dependent field becomes shorter by a factor of 400.

2.3. Polarization and Asymmetry

It is believed that there is no depolarization in the stopping stage of muons because the Coulomb interaction is dominant. Thus the positive muon has full initial polarization. On the other hand, the negative muon forms a muonic atom, in which a large depolarization due to the spin orbit coupling takes place [7] and thus the resultant polarization at the 1s ground state is around 1/6. This estimate is based on various assumptions on the capture stage of the muon. (This depolarization may depend on the atomic number Z, because the population of ℓ at the capture stage depends on Z and does not seem to follow the statistical distribution [8]). Since the earlier stage of the muonic cascade causes Auger excitations of atomic electrons, there could be further depolarization if such atomic excitations are not recovered quickly enough. In metals there should be no such depolarization, and even in insulators like sulphur the polarization is often preserved. This problem is open to further investigation.

2.4. Lifetime and electron yield

The lifetime determines the natural time window for the hyperfine phenomena. While the positive muon has a free mean life of 2.2 μsec, the bound muon has a shorter lifetime because of the competing decay branch for muon capture. In lightest elements it is still around 2 μsec and drops down rapidly with increase of Z and reaches around 80 μsec for $Z \gtrsim 40$ as shown in Fig. 1. This also means a very small electron yield compared to the positive muon. The precision due to statistics is [6].

$$\frac{\Delta\omega}{\omega} = \frac{\sqrt{2}}{\omega\tau A\sqrt{N}} \tag{6}$$

and thus precision measurements become very difficult for $Z > 20$.

2.5. Location and Size

The positive muon behaves like a proton. It sometimes forms a bound state with an electron (so-called muonium). Its location is interstitial and spread

over a wide region, even hopping over different interstitial sites by thermal diffusion. This is a very interesting and important characteristic of μ^+SR.

The negative muon is trapped by a nucleus of charge Ze at a site. It forms a dilute impurity atom because the muonic atom looks a pseudo nucleus of charge (Z-1)e when viewed from atomic electrons. However, the charge distribution of the muonic atom is different from that of the nucleus of charge (Z-1)e, as shown in Fig. 2. Furthermore, its magnetization distributes over the muon density $|\Psi_\mu(r)|^2$.

The spatial density of the bound muon is, for a point nucleus of charge Ze,

$$|\Psi_\mu(r)|^2 \simeq \frac{1}{\pi a_\mu^3} e^{-2r/a_\mu} \tag{7}$$

where the muon Bohr radius is

$$a_\mu = \frac{260}{Z} \text{ fm} \tag{8}$$

which is appreciably greater than the nuclear radius R_o. It is even an underestimate because of the finite size. Thus, the muonic atom has a charge distribution considerably different from those of the nucleus of charge (Z-1)e, and a large hyperfine anomaly [9] may be expected.

2.6. Scaling law

In the absence of hyperfine anomaly the following relations hold:

$$F_1 \equiv \frac{(\omega/g)_{muon}}{(\omega/g)_{nucleus}} \to 1 \tag{9}$$

$$F_2 \equiv \frac{(g^2T_1T)^{-1}_{muon}}{(g^2T_1T)^{-1}_{nucleus}} \to 1 \tag{10}$$

Namely, the relaxation rate for the bound muon is 400 times greater than the typical nuclear spin relaxation rate. The muon is thus very sensitive to the fluctuation of the hyperfine field and could perhaps be too sensitive to detect any observable asymmetry in some cases.

3. Instrumentation

The experimental set up of μ^-SR experiments at LBL is shown in Fig. 3. We used a 9 inch Varian magnet of 3 inch gap and applied magnetic field up to 10 kGauss over a typical target dimension of 2" x 3". The counter telescope system is a conventional one. We employed the fast logics as follows:

$$\text{"stopped } \mu\text{"} = B\cdot M\cdot S1\cdot \overline{(S2X + A1 + A2)} \tag{11}$$

$$\text{"decay e"} = S2X\cdot S2\cdot E\cdot S3\cdot \overline{(B + M + S1 + A1 + A2)} \ . \tag{12}$$

The time interval between a stopped muon and a decay electron was measured by means of a digital counter to a precision of 0.1 nsec and this counter was connected to a PDP-15 computer. The overall time resolution was 0.5 nsec. The stopped muon rate in the target was about 5×10^3 sec^{-1}. It was essential to minimize the accidental coincidence rate associated with the μ-e time distribution, because it increases not only flat background but also background of a characteristic frequency of the microscopic burst of the beam. To this end the stopped muon signal and the decay electron signal have to be genuine. The anticoincidences in the above logics turned out to be essentially important. Nevertheless, the time distribution for heavy elements involved considerable background. In addition, it generally involves background of 2 μsec mean life due to the carbon in the neighboring plastic counters.

Figure 4 shows a typical time distribution for a Mo target. It is difficult for an eye to tell the Larmor frequency in it because of the small amplitude and high frequency. Fig. 5 shows a χ^2 fitting of the time distribution to an appropriate function involving the Larmor frequency as a parameter in the case of a graphite target. Despite the small amplitude it is thus easy to determine the frequency for light elements. However, for heavy elements it becomes difficult because of the shorter lifetime and smaller yield. An example for Zn metal is shown in Fig. 6.

4. G Factors of Bound Muons

In 1928, following the Dirac theory of the electron, Breit[10] predicted the following change of the g factor of the electron in a K shell due to its relativistic motion:

$$\frac{\delta g}{g} = -\frac{1}{3}(\alpha Z)^2. \tag{13}$$

While this effect was not examined in ordinary atoms because of the lack of techniques to measure the g factors of deeply bound electrons, it is straightforward to study this effect in the ground states of muonic atoms which consist of one muon in the $s_{1/2}$ state and a zero-spin nucleus. The first observation of the Breit effect was done in 1961 by Hutchinson et al.[11] who determined the g factors of the bound muons in light elements up to Z = 16. Their values agreed well with the estimate of Breit. At the same time Ford et al.[12] made a comprehensive calculation of all the possible effects on the bound-muon g factors. The largest is the binding correction due to the Breit effect, which, however, shows considerable deviation from the point nucleus

estimate (13) of Breit starting around Z = 16, because of the finite nuclear size. It was obviously interesting and also important to extend such measurements to heavier nuclei, where greater effects were expected, but it became exceedingly difficult to determine the g factors precisely because of the shorter lifetimes and the smaller yields of decay electrons. Experiments on the diamagnetic metals of Zn, Cd and Pb were performed for this purpose [13]. Already Ignatenko et al. [14] observed spin precessions in these metals but obtained no accurate precession frequencies.

Possible corrections on the effective field at the bound nuon are for the Knight shift and the diamagnetic shielding. After these corrections the final experimental values are plotted and compared with the theoretical values of Ford et al. in Fig. 7. This experiment supports the finite size calculation of Ford et al.

5. Relaxation Phenomena in Transition Metals

The earlier work by the Dubna group [15] showed absence of the asymmetry for transition metals of Cr, Mo and Pd. They ascribed this fact to relaxation due to the paramagnetism. Since the Dubna experiment was to detect the asymmetry only for the free muon frequency, their results would indicate either that the relaxation time should be shorter than 100 nsec or that the frequency is shifted considerably. In any case, this fact seems to be surprising in view of the known nuclear spin relaxation times and Knight shifts [16-19]. If we convert $(T_1T)_{nucleus}$ into $(T_1T)_{muon}$ according to the relation (10), we expect

$$(T_1T)_{\mu^-Mo} = 4.2 \text{ msec} \cdot \text{deg.} \tag{14}$$

The Dubna result would indicate $F_2 \gtrsim 100$! In order to investigate this surprising problem we performed time differential measurements on Mo metal at two temperatures (18 and 300 k) [20]. Fig. 8 shows χ^2 fitting, where almost free frequency is clearly revealed both at T = 18 and 300 K. The Knight shift for μ^-Mo turned out to be small:

$$K(\mu^-Mo) = 0.9 \pm 1.5\% \tag{15}$$

which agrees with that for Nb in Mo [17]. Our result is thus in disagreement with the Dubna result and shows that μ^-Mo may not be so different from the Nb probe. However, the small value of $K(\mu^-Mo)$ does not exclude a large F_2, since the Knight shift in Mo metal consists of three small contributions of different signs (K_s: positive, due to 5s contact electron; K_d: negative, due to core

polarization by 4d electron; and K_{orb}: positive, due to orbital field of 4d electron). On the other hand, the large negative Knight shift observed for Rh in Pd metal by Rao et al.[18] is mostly due to the core polarization. Therefore, μ^-Pd would be a nice case where a hyperfine anomaly associated with the inner shell core polarization [21] can be observed.

We tried to measure μ^-Pd precession at 30 K and 4.2 K, but this did not show any distinct dip in the χ^2 plot. This seems to be strange, because, if one extrapolates and converts the known T_1 at 4.2 K for Rh in Pd [19] into our case, one expects $T_1(\mu^-\text{Pd})$ at 4.2 K to be 16 μsec. The present result may infer following possibilities: 1) a large hyperfine anomaly (enhanced) for the static shift and/or for the relaxation process and 2) depolarization takes place during the processes of slowing down, capture or cascade.

We tried to measure μ^-SR in the paramagnetic Ni metal with a hope to find paramagnetic Knight shifts and to study critical fluctuation phenomena and also to measure the internal field in its ferromagnetic phase. However, so far no signal has been found at T = 700 and 910 K (the T_C of Ni is 631 K). One can deduce the correlation time τ_c from the relation

$$\frac{1}{T_2} = 2\omega_{hf}^2 \tau_c \frac{S+1}{S} \tag{16}$$

by assuming that ω_{hf} is the same as that for Co in ferromagnetic Ni (H_{hf} = 120 kG). The correlation times thus obtained are $\gtrsim 5 \times 10^{-4}$ sec. The correlation times deduced from the PAC in Rh<u>Ni</u> by Gottlieb and Hohenemser [22] are plotted in Fig. 9. Extrapolation of the latter data to higher temperatures would give much shorter τ_c, but in this high temperature region the correlation time is believed to reach a limiting value set by the exchange interaction ($\approx 10^{-14}$ sec). Therefore, our data are not inconsistent with the Rh<u>Ni</u> data, and possibility to observe μ^-Ni precession looks just marginal. This discussion will give some idea about the limitation of the μ^-SR method; namely, it is difficult to handle internal field more than 100 kG.

In connection with this study the Tokyo-LBL collaboration group studied μ^+ spin relaxation in paramagnetic Ni [23]. Assuming that the hyperfine field at μ^+ observed in ferromagnetic Ni, which is only -0.66 kG [24], is responsible for the relaxation, one expects relaxation times longer than a few μsec, but very fast relaxation was observed even at high temperatures. This simply indicated that the μ^+ in paramagnetic Ni should feel a much stronger field fluctuation. One candidate is the dipolar field from neighboring Ni, which

does not appear in the ordered phase because of the cubic symmetry of the μ^+ site in Ni, but now contributes additively at high temperatures because of random orientations of the spins. At intermediate temperatures the field may be reduced because of the possible collective motion. However, the observed relaxation rates are even much shorter than expected for such random dipolar interactions [25], if one uses the τ_c derived from PAC in Rh-Ni by Gottlieb and Hohenemser. This is a very interesting problem.

6. Possible other problems

6.1 Light elements.

In contrast to heavy elements, studies of light elements, such as C and O, are rather easy from the view point of counting statistics. In addition to the easiness, the situation that the carbon and oxygen elements are very difficult to study by the conventional NMR method is even encouraging. Depolarization phenomena in organic substances have been studied by the Dubna group [5]. We are trying to study oxides of transition elements. Here, the largest problem is whether such compound (mostly insulators) can preserve the initial polarization or not, because the quenching may take place slowly. In such cases, the magnetic resonance method will be superior, as a longitudinal field may help holding the polarization. Another problem is possible quick damping of the asymmetry due to the dipolar field broadening. Although μ^-O is not troubled by any quadrupole field, it may well have a considerable field broadening when located in a non-cubic site. Therefore, use of a single crystal is most desirable.

6.2. Semiconductors

For instance, μ^-Si is a very nice dilute acceptor in a Si crystal. At room temperatures, both p type and n type Si crystals showed a full precession of free frequency. At low temperatures we expect that the acceptor, μ^-Si, will trap a hole to form a hydrogen-like bound state, and show a quite different frequency spectrum corresponding to a modified Breit-Rabi energy scheme.

6.3. Weak ferromagnetism

Probably μ^-SR is most suited to studies of weak ferromagnetism. One can study, for instance, the internal fields at Zn and Zr in $ZrZn_2$. Such a project is also under way.

At the moment our experiments are troubled by a low beam polarization and high electron background at the μ^- channel. We are very confident that the future facilities at meson factories which are coming up now will be very powerful for

performing μSR physics. We would like to persuade solid-state physicists to come into this field.

We would like to thank Professors K. M. Crowe and O. Chamberlain for the pleasant collaboration and hospitality at Lawrence Berkeley Laboratory.

Reference and footnote

†Work supported by Japan Society for the Promotion of Science, the National Science Foundation, and the Mitsubishi Foundation; invited talk presented by T. Yamazaki at the International Conference on Hyperfine Interactions Studied in Nuclear Reactions and Decay, Uppsala, June 10, 1974.

1. Garwin, R. L., Lederman, L. M., and Weinrich, M., Phys. Rev. 105, 1415 (1957).
2. Lundby, R. A., Sens, J. C., Swanson, R. A., Telegdi, V. L., and Yovanovitch, D. D., Phys. Rev. Lett. 1, 38 (1958); Garwin, R. L., Hutchinson, D. P., Penman, S., and Shapiro, G., Phys. Rev. 118, 271 (1960).
3. Coffin, T., Garwin, R. L., Lederman, L. M., Penman, S., and Sachs, A. M., Phys. Rev. 106, 1108 (1957).
4. Brewer, J., Crowe, K. M., Schenck, A., and Gygax, F., to be published in "Muons" (ed. Wu, C. S., and Hughes, V. W.).
5. Evseev, V. S., to be published in "muons" (ed. Wu, C. S., and Hughes, V. W.)
6. Crowe, K. M., Hague, J. F., Rothberg, J. E., Schenck, A., Williams, D. L., Williams, R. W., and Young, K. K., Phys Rev. D5 2145 (1972).
7. Mann, R. A., and Rose, M. E., Phys. Rev. 121, 293 (1961); see also Ref. 5).
8. This conjecture is inferred from: Wiegand, C. E., and Godfrey, G. L., Phys. Rev., to be published.
   Quitman, D., Engfer, R., Hegel, U., Brix, P., Backenstoss, G., Goebel, K., and Stadler, B., Nucl. Phys. 51, 609 (1964).
   Ponomarev, L. I., Ann. Rev. Nucl. Sci. 23, 395 (1973).
   Leon, M., and Seki, R., Phys. Rev. Lett 32, 132 (1974).
   Hoff, D. K., Vogel, P., and Winther, A., to be published.
9. Bohr, A., and Weisskopf, V. F., Phys. Rev. 77, 94 (1950). Stroke, H. H., Blin-Stoyle, R. J., and Jaccarino, V., Phys. Rev. 123, 1326 (1961); Rosenberg, H. J., and Stroke, H. H., Phys. Rev. A5, 1992 (1972). Otten, E. W., Z. für Physik, 225, 393 (1969).
10. Breit, G., Nature 122, 649 (1928).
11. Hutchinson, D. P., Menes, J., Shapiro, G., Patlach, A. M., and Penman, S., Phys. Rev. Lett. 7, 129 (1961); Hutchinson, D. P., Menes, J., Shapiro, G., and Patlach, A. M., Phys. Rev. 131, 1362 (1963).
12. Ford, K. W., Hughes, V. W., and Wills, J. G., Phys. Rev. Lett. 7, 134 (1961); Phys. Rev. 129, 194 (1963).

13. Yamazaki, T., Nagamiya, S., Hashimoto, O., Nagamine, K., Nakai, K., Sugimoto, K., and Crowe, K. M., LBL-2666 (March 1974), to be published.
14. Ignatenko, A. E., Egorov, L. B., Khalupa, B., and Chultem, D., Soviet Physics JETP 8, 792 (1958).
15. Egorov, L. B., Zhuravlev, G. V., Ignatenko, A. E., Syuang-Ming, Li, Petrashku, M. G., and Chultem, D., Nucl. Phys. 23, 62 (1961); Ignatenko, A. E., Nucl. Phys. 23, 75 (1961).
16. Narath, A., and Alderman, D. W., Phys. Rev. 143, 143 (1966).
17. Masuda, Y., and Nishioka, M., J. Phys. Soc. Japan 22, 238 (1967).
18. Rao, G. N., Matthias, E., and Shirley, D. A., Phys. Rev. 184, 325 (1969).
19. Narath, A. and Weaver, H. T., Phys. Rev. 3B, 616 (1971).
20. Yamazaki, T., Nagamine, K., Nagamiya, S., Hashimoto, O., and Kobayashi, S., private communication, 1974.
21. Freeman, A. J., and Watson, R. E., in "Magnetism" Vol. IIA (ed. Suhl, H., and Rado, G., Academic Press, Inc., New York, 1965).
22. Gottlieb, A. M., and Hohenemser, C., Phys. Rev. Lett. 31, 1222 (1973).
23. Nagamine, K., and Patterson, B., private communication, 1974.
24. Patterson, B. D., Crowe, K. M., Gygax, F. N., Johnson, R. F., Portis, A. M., and Brewer, J. H., Phys. Lett. 46A, 453 (1974).
25. Portis, A. M., private communication, 1974.

Table I.

Characteristic features of μ^+SR and μ^-SR

	μ^+	μ^-
Spin	1/2	1/2, when bound to I = 0 nucleus
g factor	2.002 in μ_μ	a little smaller
Polarization	100%	∿18%
Asymmetry	1+ 0.33 cosθ	1+ 0.06 cosθ
Lifetime	2.2 μsec	2.2 μsec ∿80 nsec with Z
Electron yield	100%	100% ∿4% with Z
Location	interstitial	at nucleus
Size	diffusing	$a_\mu \sim \frac{260}{Z}$ fm
Character	light proton	pseudo nucleus of (Z-1)e

Figure Captions

Fig. 1. Mean lifetimes and decay electron branches of the muonic $1s_{1/2}$ state versus the atomic number Z of the nucleus to which the negative muon is bound.

Fig. 2. Charge distribution of the muonic atom $\mu^- Z$, as compared with that of an equivalent nucleus of charge (Z-1)e.

Fig. 3. Experimental setup for $\mu^- SR$ at the 184" cyclotron of Lawrence Berkeley Laboratory. All the counters were plastic scintillators connected to RCA 8575 phototubes through photoguides. These counters were placed between two pole pieces of the 9-inch Varian magnet with its gap of 7.6 cm. The A1 and A2 counters (3 mm thick) were fixed to the surfaces of the pole pieces in order to eliminate the background from the iron cores.

Fig. 4. Typical time distribution of $\mu^- e$ decay in Mo.

Fig. 5. χ^2 versus the Larmor frequency for $\mu^- C$ (graphite)

Fig. 6. χ^2 versus the Larmor frequency for $\mu^- Zn$ (metal).

Fig. 7. Relativistic effect (or binding effect) on the g factor of bound muons. The dotted curve shows the relativistic correction for a point nucleus[10]. The solid curve shows the calculated values by Ford et al. [12] where the finite size effect of the nucleus is taken into account. The difference between the solid and broken curves is the nuclear polarization effect calculated by Ford et al. The experimental data after the corrections for the Knight shift and diamagnetism are plotted.

Fig. 8. χ^2 versus the Larmor frequency for $\mu^- Mo$ (metal at 18 and 300 K).

Fig. 9. Correlation times in paramagnetic Ni as deduced from PAC in Rh-Ni by Gottlieb and Hohenemser. [22] Two lower limits set by $\mu^- Ni$ are given.

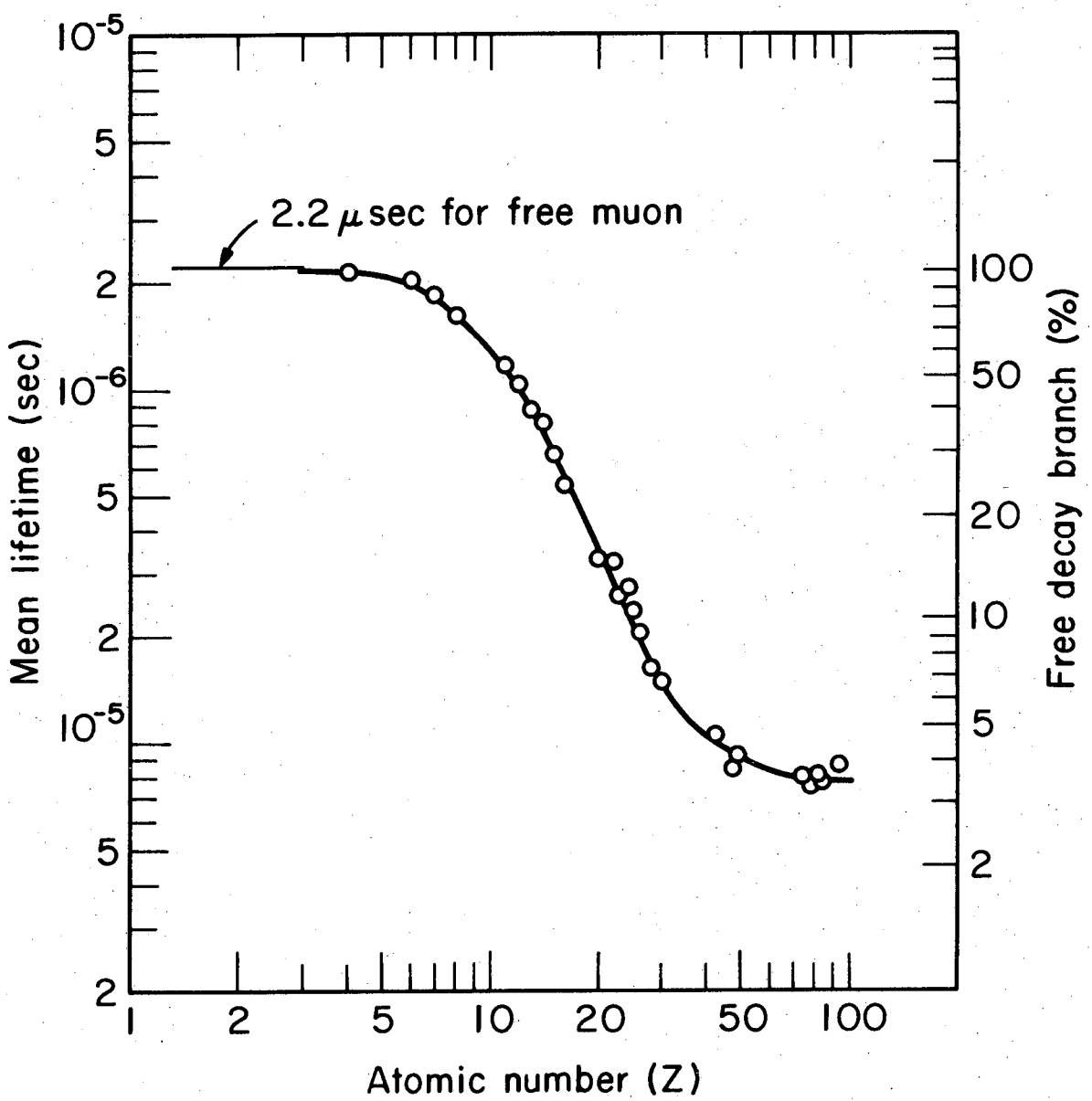

XBL 747-3587

Fig. 1.

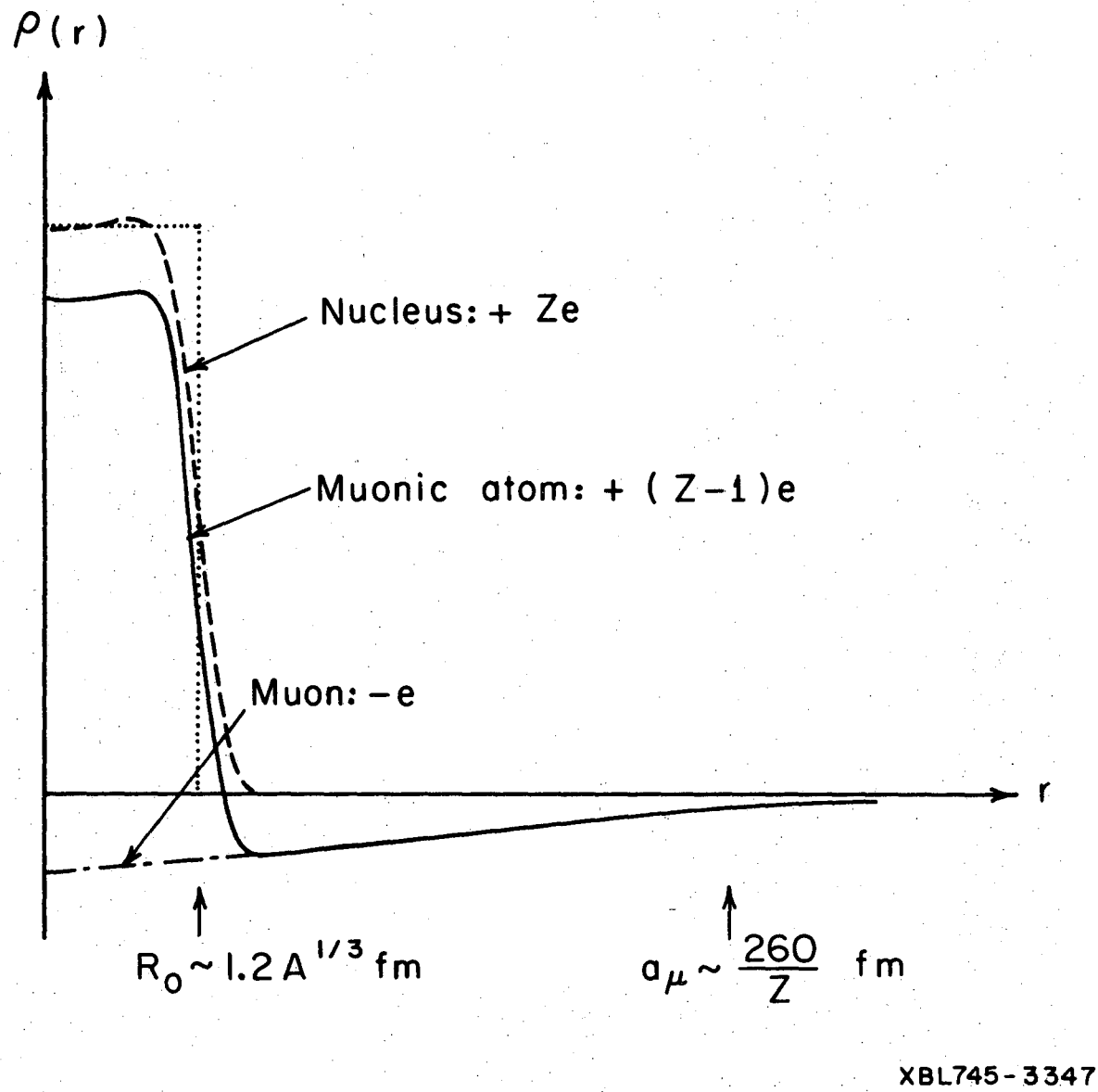
ρ(r)
Nucleus: + Ze
Muonic atom: + (Z−1)e
Muon: −e
r
$R_0 \sim 1.2 A^{1/3}$ fm
$a_\mu \sim \frac{260}{Z}$ fm
XBL745-3347

Fig. 2.

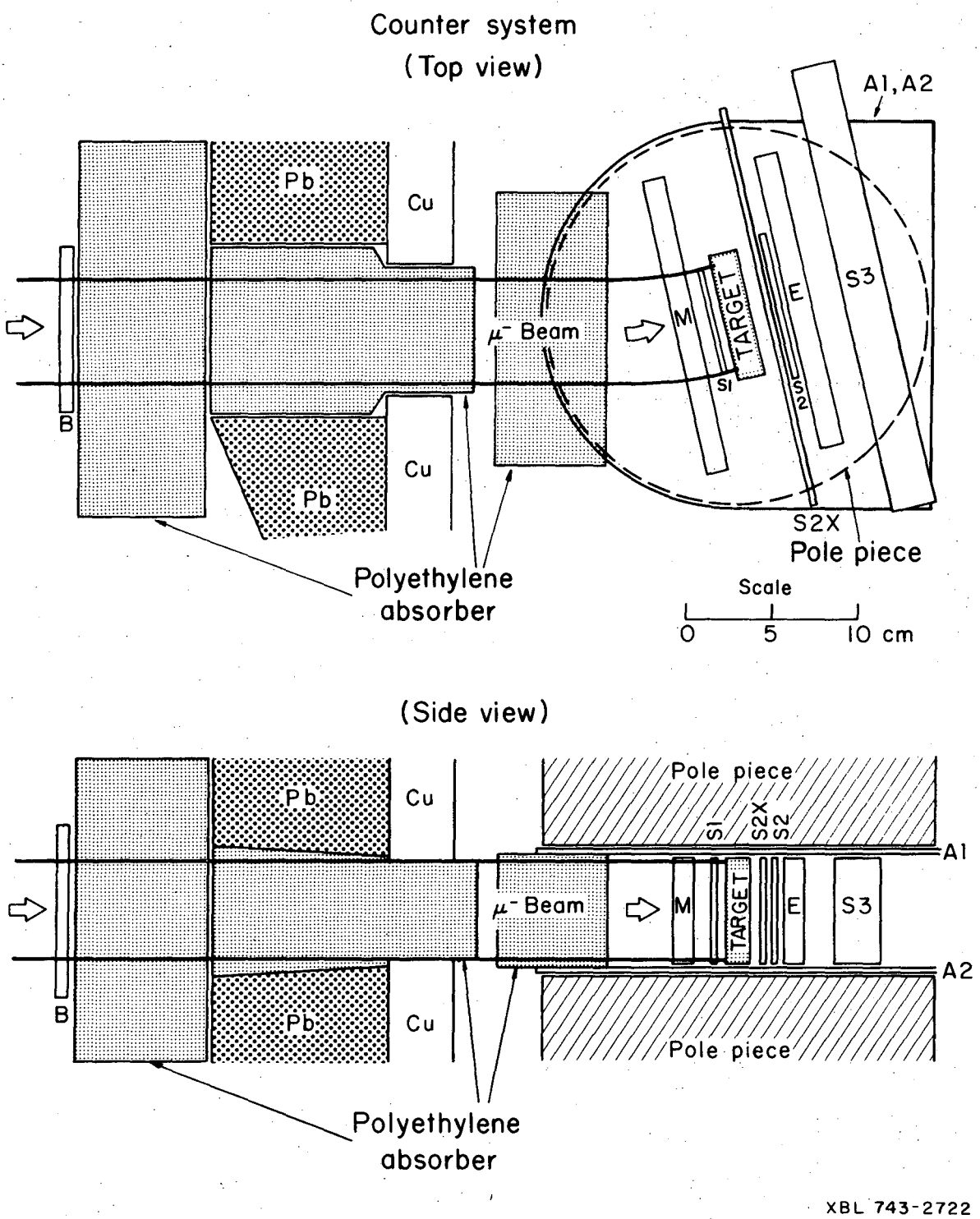
Counter system
(Top view)
A1, A2
Pb
Cu
B
μ⁻ Beam
M
TARGET
E
S3
S1
S2
S2X
Pole piece
Polyethylene
absorber
Scale
0 5 10 cm
(Side view)
Pb
Cu
Pole piece
S1
S2X
S2
A1
μ⁻ Beam
M
TARGET
E
S3
A2
B
Pb
Cu
Pole piece
Polyethylene
absorber
XBL 743-2722

Fig. 3.

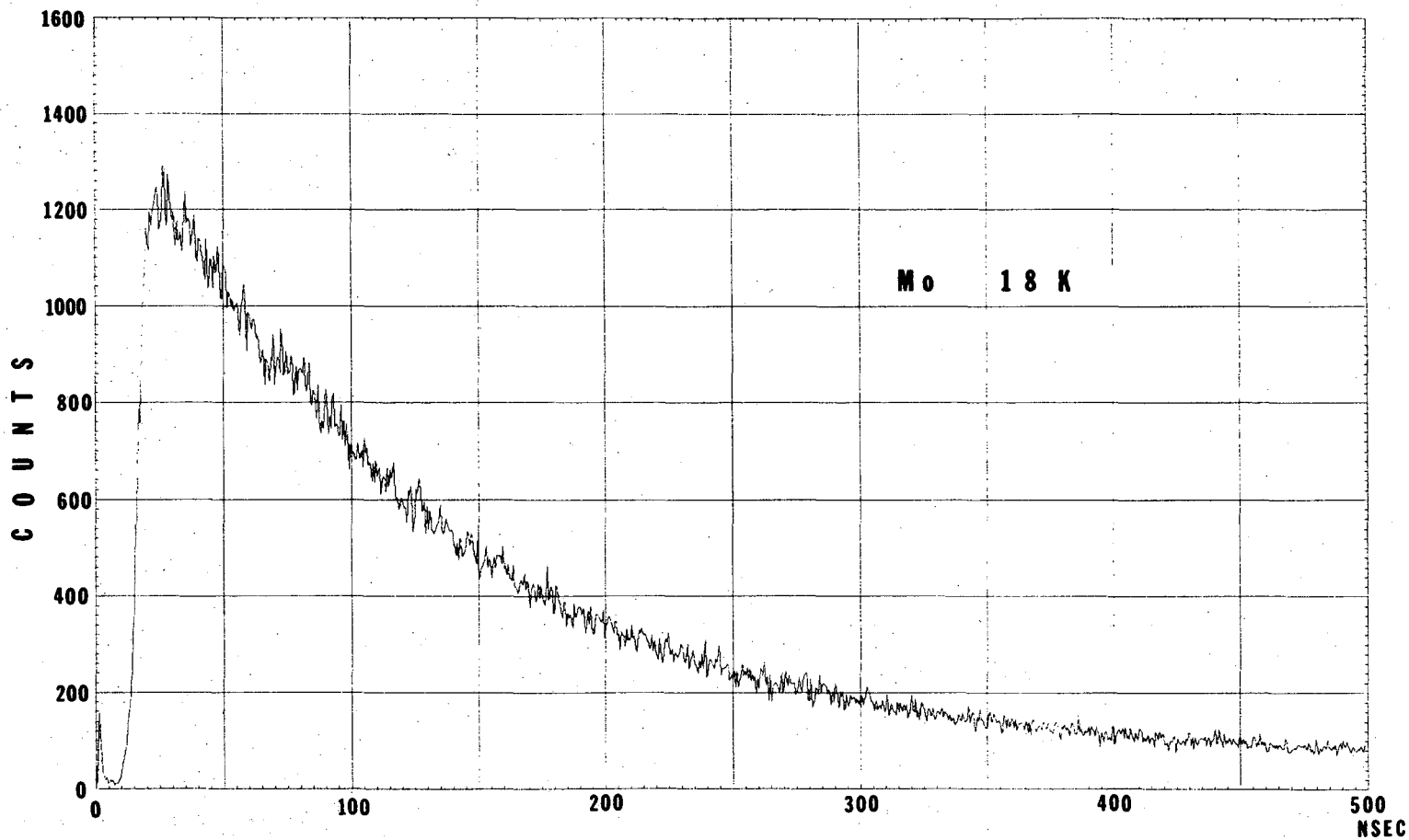

XBL 747-1166

Fig. 4.

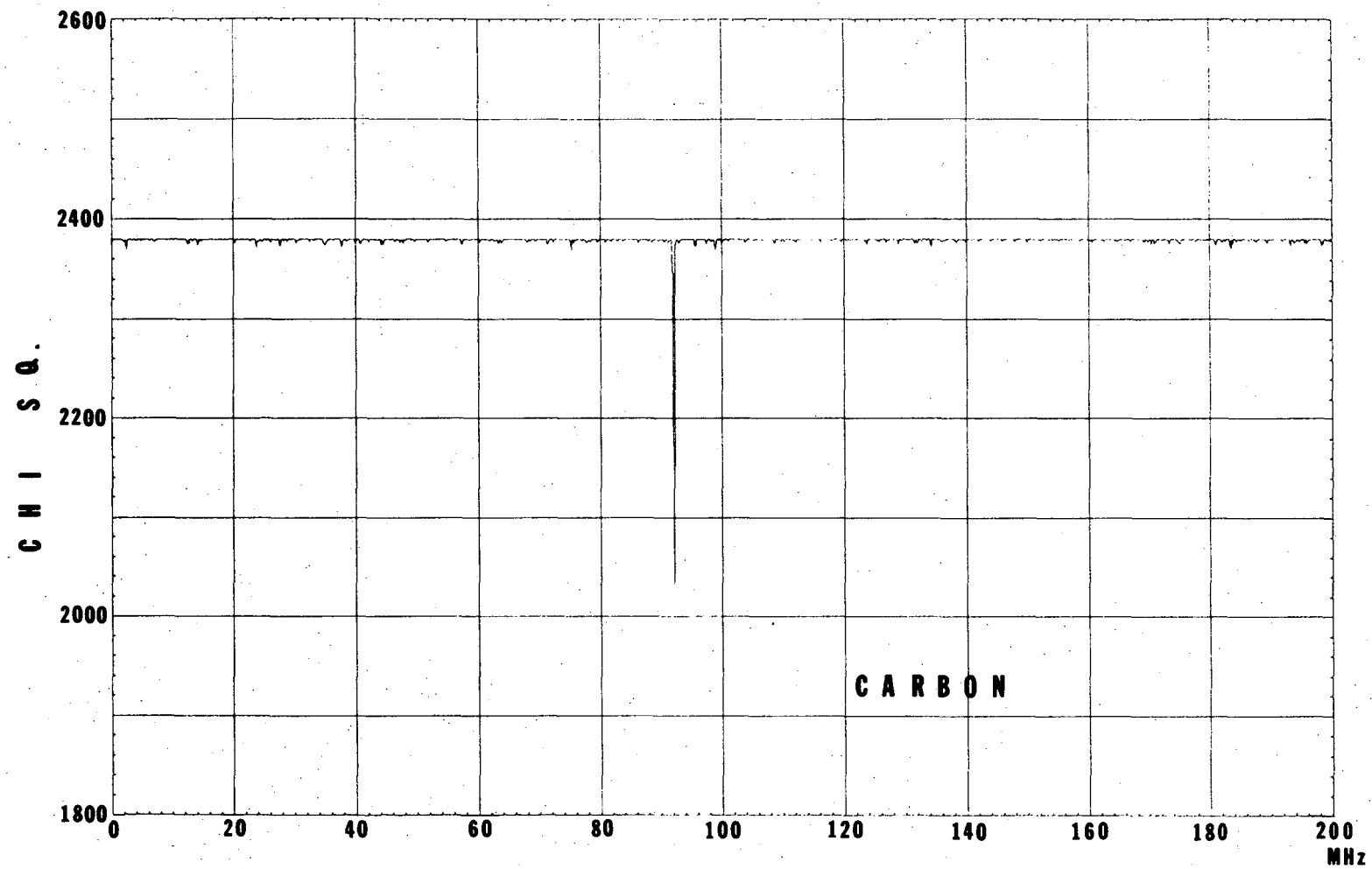

XBL 746-982

Fig. 5.

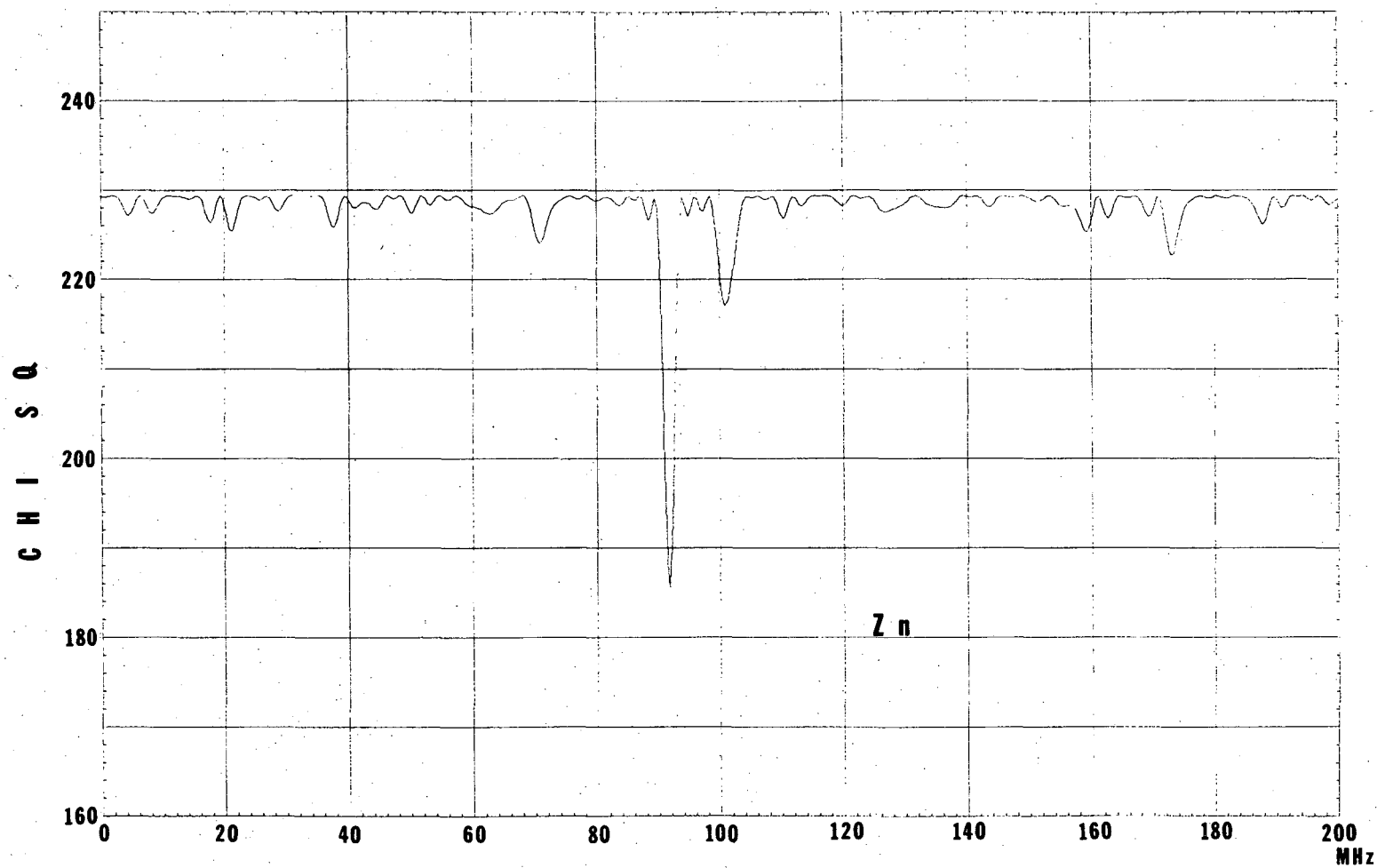

XBL 747-1167

Fig. 6.

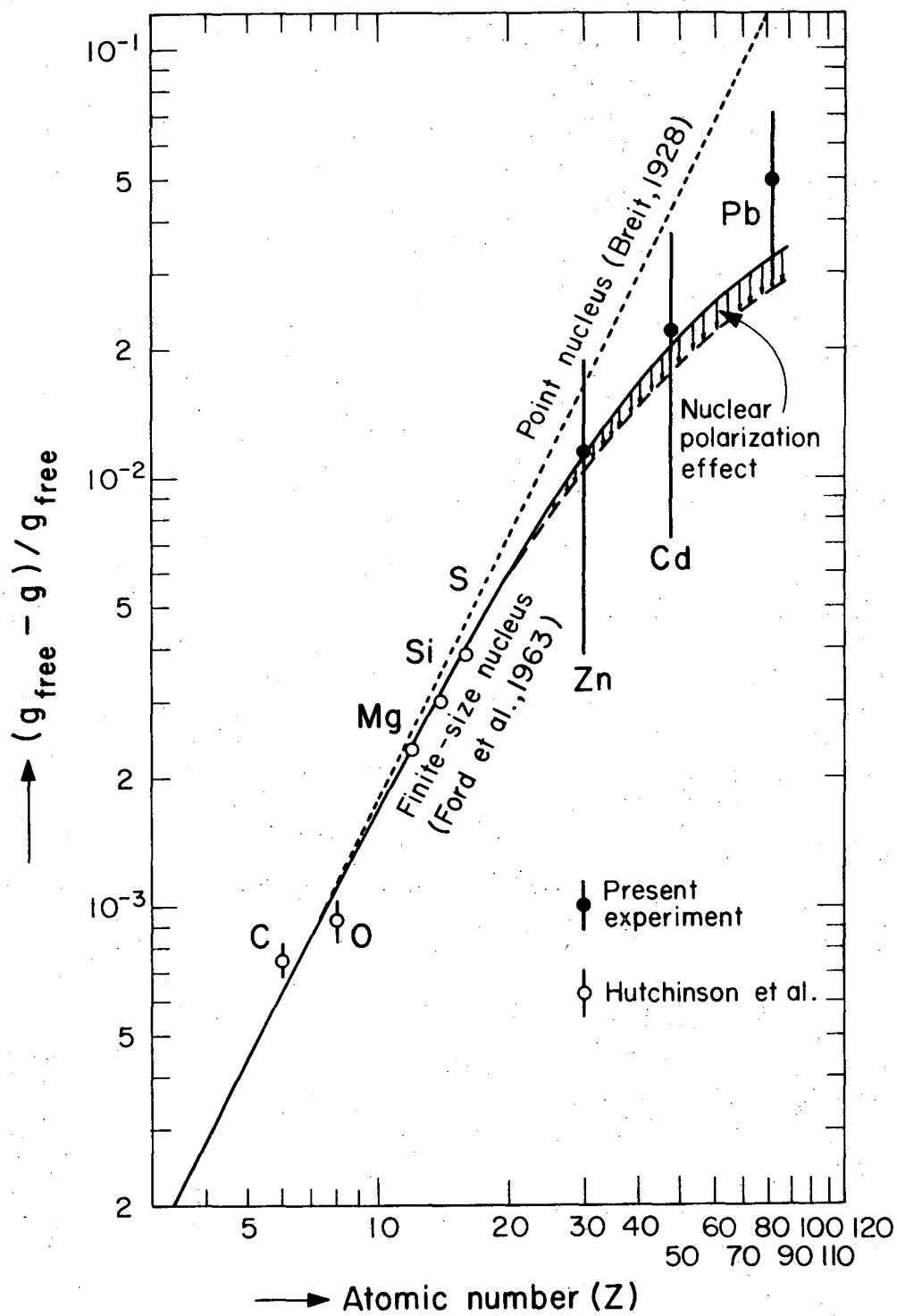

XBL 743-2706

Fig. 7.

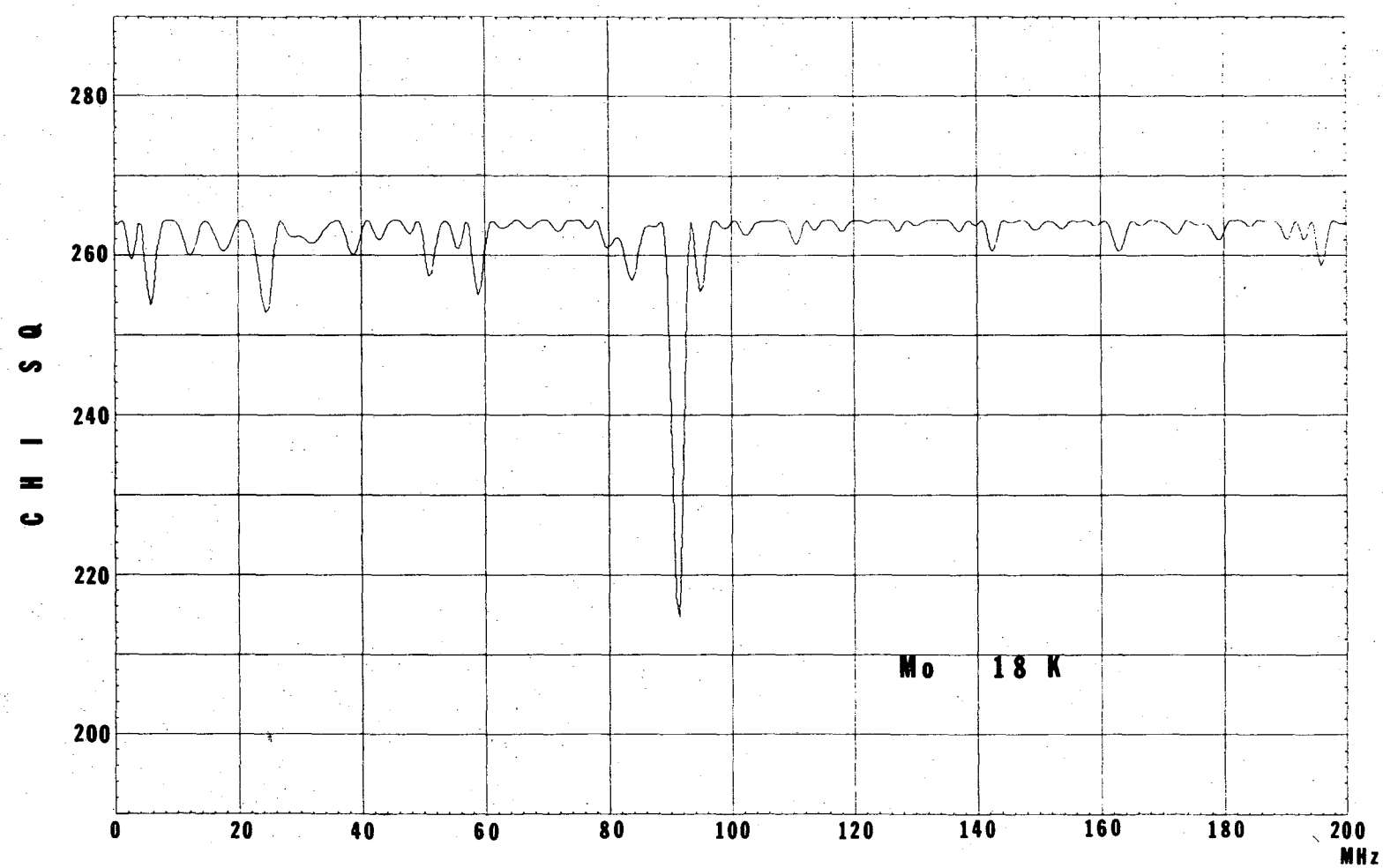

XBL 746-981

Fig. 8.

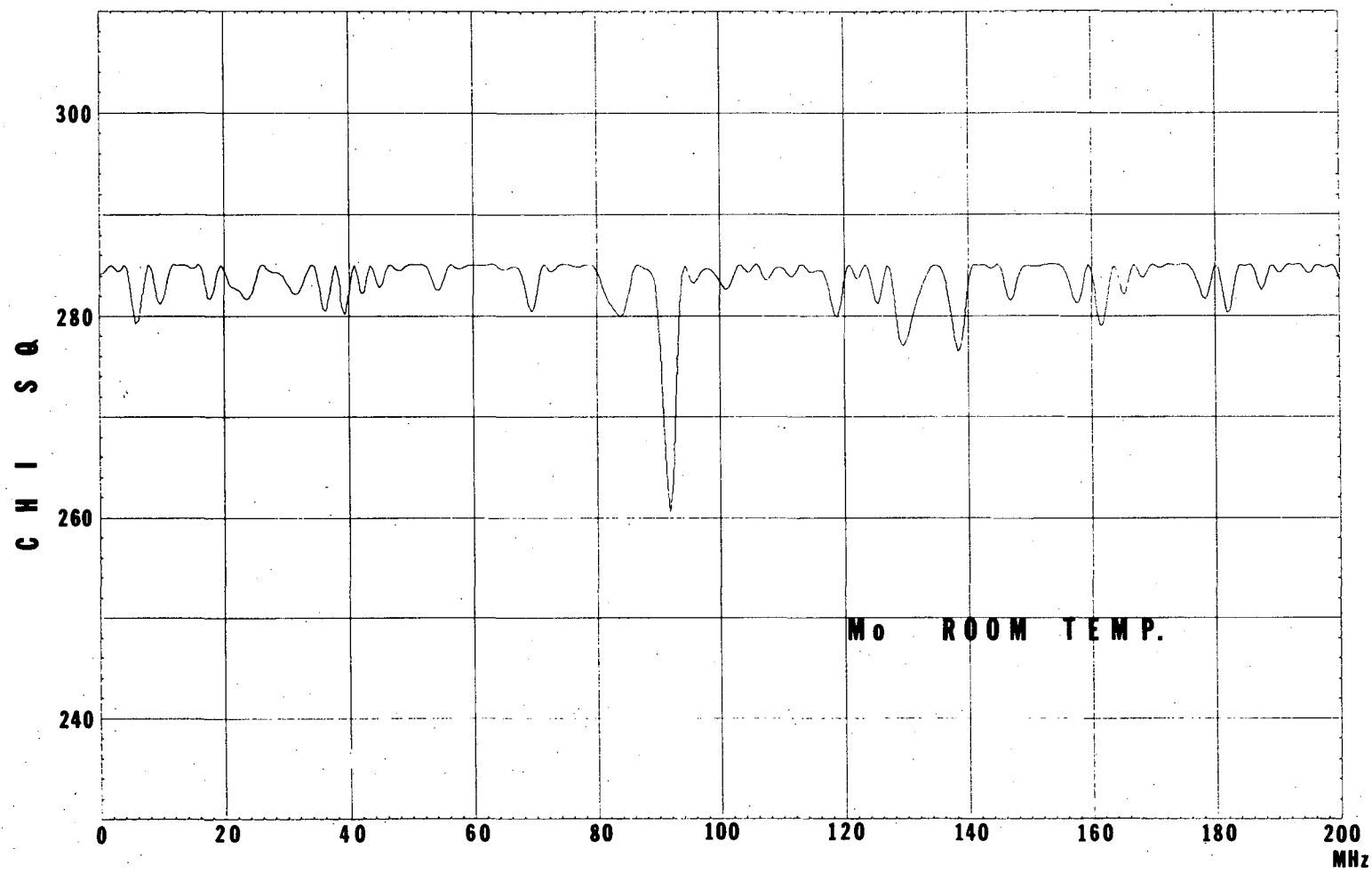

XBL 746-980

Fig. 9.

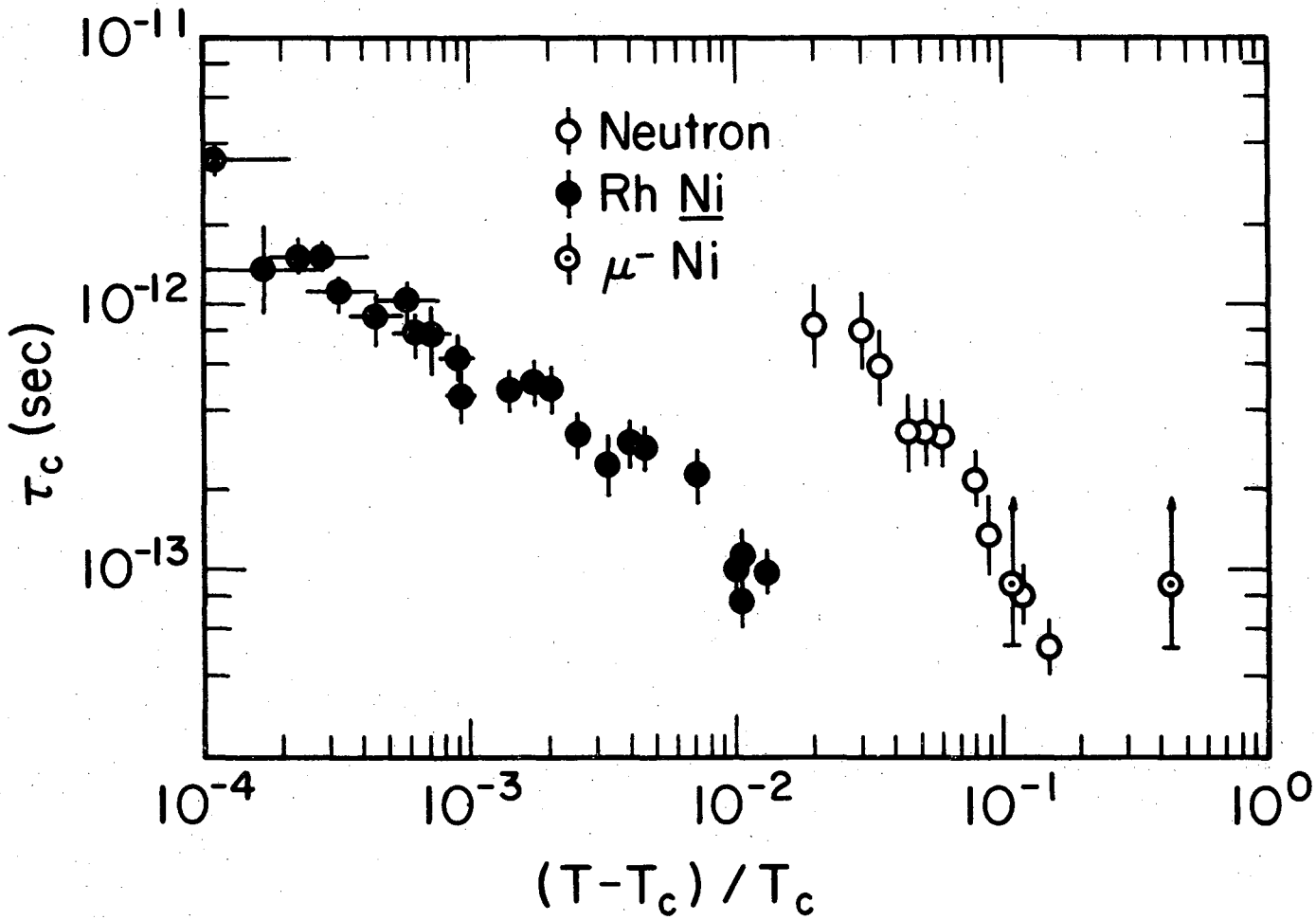

XBL 747-3586

Fig. 10.

LEGAL NOTICE

This report was prepared as an account of work sponsored by the United States Government. Neither the United States nor the United States Atomic Energy Commission, nor any of their employees, nor any of their contractors, subcontractors, or their employees, makes any warranty, express or implied, or assumes any legal liability or responsibility for the accuracy, completeness or usefulness of any information, apparatus, product or process disclosed, or represents that its use would not infringe privately owned rights.

TECHNICAL INFORMATION DIVISION
LAWRENCE BERKELEY LABORATORY
UNIVERSITY OF CALIFORNIA
BERKELEY, CALIFORNIA 94720